46th Annual Review of Progress
in Quantitative Nondestructive Evaluation
QNDE2019
July 14-19, 2019, Portland, OR, USA

QNDE2019-6935

ULTRASONIC IMMERSION TESTING FOR DEPTH SIZING OF CRACK-LIKE DEFECTS IN LARGE DIAMETER PIPES

Rosen K. Rachev[1,2,*], Alexander Velichko[1], Paul Wilcox[1]
1. Department of Mechanical Engineering, University of Bristol, Bristol, United Kingdom
2. Baker Hughes, a GE company, United Kingdom

ABSTRACT

Detection and depth sizing of surface breaking defects in large diameter pipes is of vital importance in the petrochemical industry. An analytical forward model is presented and used to simulate ultrasonic phased array data in an inspection geometry close to that experienced by a pipeline inspection gauge. The data has been imaged with Total Focusing Method (TFM) and Plane Wave Imaging (PWI). Image-based depth sizing has been applied using a minimum bounding box around pixels above a threshold intensity. Initial results are presented from a half-skip transverse wave imaging and sizing of crack-like defects of depths between 1 and 6 mm and orientation angles between –25° and 25°. TFM results show good agreement with nominal values in the –10° to 10° angular range for all depths. PWI outputs similar results with less than a sixth of the data.

Keywords: non-destructive evaluation, pipe inspection gauge, ultrasonic, imaging, depth sizing.

1. INTRODUCTION

In the petrochemical industry, the integrity of pipelines, tanks and pressure vessels is paramount because potential spills are environmentally toxic and costly to repair. Ultrasonic non-destructive evaluation (NDE) is often a suitable solution for their inspection. However, undertaking this process manually poses a few issues. Covering a substantial area is costly and requires a significant amount of time. Additionally, undesirable alterations might be necessary to the operation of the inspected equipment ranging from removal of insulation to complete plant shutdown. Recently, there has been a shift towards automated inspections. Permanently installed sensors and structural health monitoring is an automated implementation that provides a continuous stream of data from a specific region [1]. If instead a larger area is to be covered, the ultrasonic sensors can be mounted onto a moving tool such as a robot crawler [2] or a pipe inspection gauge ('pig') [3].

The focus of this work is on the possible improvements of the operation of pigs. Pigs are unmanned tools that travel through a pipeline with the flow and perform local measurements as they move along. This operation is termed an in-line inspection (ILI). Historically, ultrasonic pigs have been equipped with monolithic transducers. More recently, electro-magnetic acoustic transducers have been employed to avoid coupling issues in gas pipeline inspections, and phased arrays (PAs) – to increase sensitivity to both corrosion and cracking in oil pipelines. The PAs are arranged circumferentially around the pig, emit sound in immersion through the flowing pipeline product and receive echoes from the pipe walls and possible defects. The inspection focus is on detection and characterization of corrosion and cracks running axially along the pipeline.

PAs house multiple piezo-electric elements. The main advantage of this technology is in the versatility of beam forming, allowing different inspections to be undertaken with the same equipment. Additionally, the full matrix capture (FMC) of data corresponding to the time domain signals from all transmit-receive element pairs can be captured. This corresponds to the full response of a defect to a PA inspection. The FMC data can be post-processed to simulate any linear inspection or to form an image. The Total Focusing Method (TFM) utilizes this complete set of time-domain data to focus at every pixel and is described as the "gold standard" for ultrasonic imaging [4]. Acquiring an FMC with an ultrasonic pig is challenging, since the tool operates at high speeds (1-2 m/s) imposing a limit on the data that can be collected at a certain location. Currently in ILI, the operation of PAs is limited to plane wave transmission and reception patterns mimicking monolithic transducers orientated at different angles. Plane Wave Imaging (PWI) is an alternative to TFM imaging technique which requires the transmission of plane waves and individual in-parallel reception on all PA elements [5]. It outputs high resolution and sensitivity images with fewer transmissions than the required by TFM and could be a viable post-processing algorithm for ILI ultrasonic data.

This paper investigates the accuracy of image-based depth sizing of crack-like defects from images formed with TFM and PWI in immersion. A forward model is described and used to simulate data on which the sizing is tested. The following sections describe the techniques and offer preliminary results.

*Contact author: rr12520@bristol.ac.uk

2. METHODS

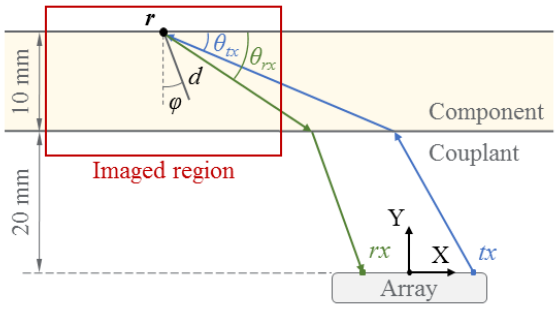

FIGURE 1: Simulation configuration and imaged region.

2.1 Forward model

Simulated PA data is useful to test an algorithm's performance for a large range of scenarios. In this work a forward model is used to simulate FMC data. The scatterer of interest is a back surface connected crack-like defect in a plate parallel to the transducer. The inspection setup is in immersion and is shown schematically in Fig. 1. The configuration is close to the real-world inspection of surface-breaking defects in large diameter pipes. The ultrasonic data received from such a defect can be modelled around a single reference point $\boldsymbol{r}$ assigned at its corner [6]. Therefore, the signal transmitted and recorded by respectively elements *tx* and *rx* is [7]:

$$G_{tx,rx}(\boldsymbol{r},\omega) = P_{tx,rx}(\boldsymbol{r},\omega)S(\theta_{tx},\theta_{rx},\omega)\Phi(\omega)e^{-i\omega T_{tx,rx}} \quad (1)$$

where ω is frequency, $P_{tx,rx}(\boldsymbol{r},\omega)$ contains the directivity, transmission and beam spreading coefficients, $S(\theta_{tx},\theta_{rx},\omega)$ is the defect scattering matrix coefficient with respect to the angles θ_{tx} and θ_{rx} formed by respectively the incident and scattered rays with the back surface, $\Phi(\omega)$ is the input signal spectrum, and $T_{tx,rx}$ is the signal travel time along the ray path. Interactions between the defect and the back surface are modelled within the scattering matrix. Direct reflections form the surfaces are not simulated. Only the mode paths used by the imaging algorithm have been simulated to reduce the presence of artifacts.

2.2 Ultrasonic imaging and defect characterization

The simulated FMC data has been processed with both TFM and PWI in the imaged region shown in red in Fig. 1. In this work, only transverse waves are modelled inside the component. The imaging is formed in transverse wave half-skip (HS) mode, with the rays from the PA towards the defect reflected by the back surface. The intensities are normalized to the maximum. The defect depth is calculated directly from the image [8]. All pixels above a –6 dB threshold are selected. Targeted pixels near one another are grouped into clusters. These clusters are the defect indications. If multiple indications are produced the one containing the highest intensity is considered to represent the defect. A minimum bounding box is fit around the representative indication and the depth is measured along the side of the box from the back surface to its tip.

3. INITIAL RESULTS AND DISCUSSION

The simulated materials are water couplant (speed of sound 1480 m/s) and carbon steel component (transverse speed 3086 m/s). The simulated PA is a 1D linear array with 5 MHz center frequency, 100 elements and pitch of 0.3 mm. The inspection configuration is specified such that a ray from the center of the PA hits the corner of the defect with a transverse wave at 45°. The simulated crack-like defects are of depths *d* between 1 and 6 mm at every 0.2 mm and angles φ from –25° to 25° at every 2° (where positive φ indicates incline towards the PA as shown in Fig. 1). The TFM image is formed from transmission and reception on all possible element pairs, while the PWI one uses 16 plane wave transmissions at angles from 30° to 60° at every 2° and reception on all elements.

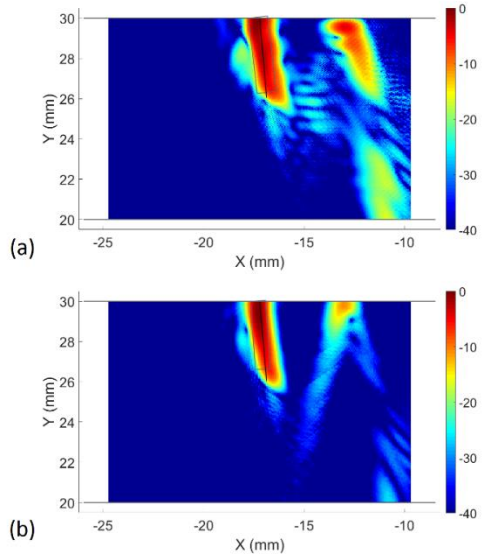

FIGURE 2: HS transverse wave (a) TFM and (b) PWI image (intensity in dB) of a defect (*d* = 4 mm, φ = 5°). The simulated defect is marked with a black line, the –6 dB bounding box is in grey. The depth measurements for TFM and PWI are respectively: 3.8 mm and 3.4 mm.

Fig. 2 shows a TFM and PWI image of the same defect (*d* = 4 mm, φ = 5°). The defect is represented sufficiently well for depth sizing purposes in both the TFM and PWI images. The measurements are respectively 3.8 mm and 3.4 mm, both within 15% of the nominal 4 mm value. Some imaging artifacts are observed at x-coordinates between –15 mm and –10 mm. Since only the relevant for imaging transverse wave paths have been simulated, those artifacts are attributed to interactions between the defect and the back surface modelled within the scattering matrix. The nominal simulated defect is represented by a black line in the images in Fig. 2. If the high intensity pixels of the actual indications are observed in the images, it is noticeable that the defect appears more inclined towards the PA than the nominal input. This is likely caused by a breakdown of the far-field assumption in eq. (1) for larger depth defects. However, the inconsistency's effect on the work is considered small, because

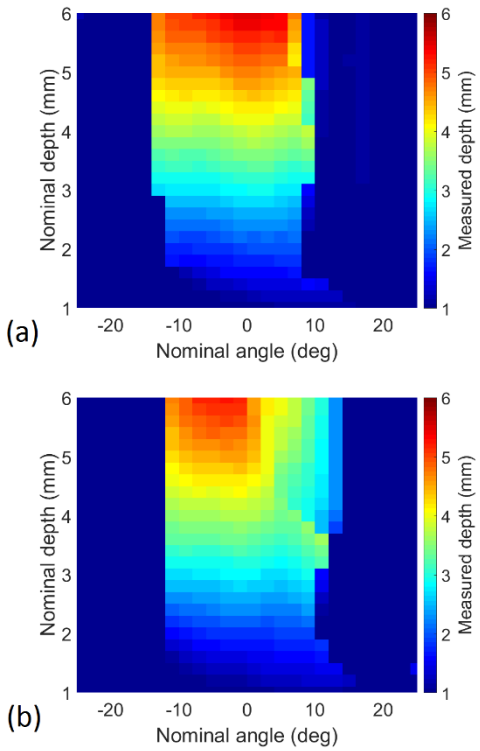

FIGURE 3: Image-based sizing summary: (a) TFM; (b) PWI

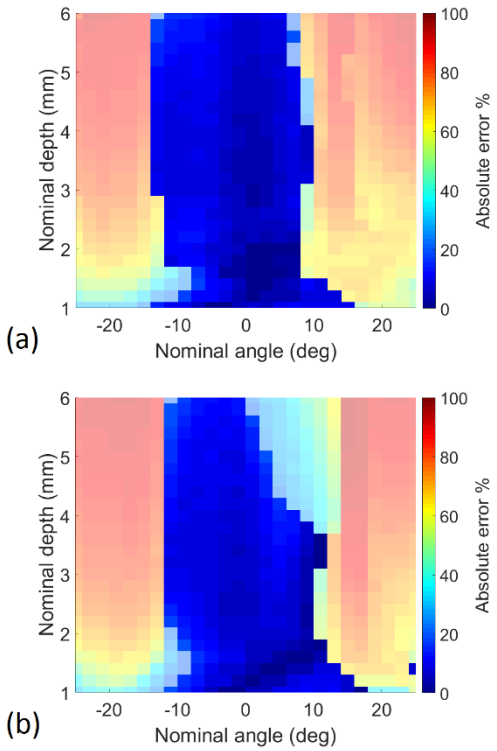

FIGURE 4: Image-based sizing error summary (20% or lower highlighted): (a) TFM; (b) PWI

the focus is on establishing the defect parameter range in which the sizing approach is viable, rather than perfectly matching simulated and experimental sizing.

A summary of the HS TFM and PWI image-based depth sizing is shown in Fig. 3, and the absolute error in percentage for the two algorithms is shown in Fig. 4, with the error lower than 20% highlighted. Image-based sizing for both algorithms outputs high accuracy results for defects with φ between –10° to 10°. Outside of this region a continuous specular reflection is no longer observed along the defect depth. To size a defect from such a pattern, the algorithm would have to rely on locating the corner and tip indications. This is not robust for real cracks as the tip reflection could be of very low amplitude and masked by noise and artifacts.

4. CONCLUSION

PWI and depth sizing based on it have been proposed as a post-processing algorithm for oil pigs PA data. A sizing summary of simulated crack-like defects has been presented. The achieved accuracy closely matches the TFM-based one, but with a sixth of the transmissions. This suggests PWI could be a viable improvement of the methods currently utilized onto oil pigs.

ACKNOWLEDGEMENTS

This work was supported by Baker Hughes, a GE company (BHGE), UK and the UK Engineering and Physical Sciences Research Council, through the UK Research Centre in NDE (RCNDE).

REFERENCES

[1] E. Dehghan-Niri and S. Salamone, “A multi-helical ultrasonic imaging approach for the structural health monitoring of cylindrical structures,” *Struct. Heal. Monit.*, vol. 14, no. 1, pp. 73–85, 2015.

[2] P. Chatzakos, Y. P. Markopoulos, K. Hrissagis, and A. Khalid, “On the development of a modular external-pipe crawling omni-directional mobile robot,” *Ind. Robot An Int. J.*, vol. 33, no. 4, pp. 291–297, 2006.

[3] D. Allen, P. Senf, I. Lachtchouk, and S. Falter, “Update on Ultrasonic Phased Array Crack Detection,” *Pipeline Gas J.*, pp. 44–50, 2010.

[4] C. Holmes, B. W. Drinkwater, and P. D. Wilcox, “Post-processing of the full matrix of ultrasonic transmit–receive array data for non-destructive evaluation,” *NDT E Int.*, vol. 38, pp. 701–711, 2005.

[5] L. Le Jeune, S. Robert, E. Lopez Villaverde, and C. Prada, “Plane Wave Imaging for ultrasonic non-destructive testing: Generalization to multimodal imaging,” *Ultrasonics*, vol. 64, pp. 128–138, 2016.

[6] A. Velichko and P. D. Wilcox, “Efficient finite element modeling of elastodynamic scattering with non-reflecting boundary conditions,” *AIP Conf. Proc.*, vol. 1430, no. 31, pp. 142–149, 2012.

[7] L. W. Schmerr, *Fundamentals of Ultrasonic Nondestructive Evaluation - A Modeling Approach*, 2nd ed. Springer International Publishing, 2016.

[8] M. V. Felice, A. Velichko, and P. D. Wilcox, “Accurate depth measurement of small surface-breaking cracks using an ultrasonic array post-processing technique,” *NDT E Int.*, vol. 68, pp. 105–112, 2014.